Langmuir

Article

pubs.acs.org/Langmuir

Chemical Passivation Processes for Biofunctionalization Schemes on Semiconductor Surfaces

Yue Liu, Junghuei Chen, and Andrew V. Teplyakov*

Department of Chemistry and Biochemistry, University of Delaware, Newark, Delaware 19716, United States

Supporting Information

ABSTRACT: In developing novel designs for semiconductor-based biosensors and for biofunctionalization of semiconductors in general, it is extremely important to be able to block the reaction sites present on a surface following the biomodification from further chemical transformations. This procedure is required both to protect the surface from oxidation and to allow for molecular-level control of the biomolecular interactions at the topmost layer. In this work, the biosensor model system is designed based on a single-strand biotin-modified thiol-DNA attached to the silicon substrate. The binding of this thiol-DNA to the surface is performed through the cross-linker sulfosuccinimidyl-4-(*N*-maleimidomethyl)-cyclohexane-1-carboxylate (SSMCC) attached to the 11-amino-1-undecene monolayer on Si(111) surface. Streptavidin-coated gold nanoparticles are used to test the reactivity of the surface and to examine the role of passivation in the entire scheme. The passivation of the remaining surface reactive sites is achieved via a reaction with 1-octadecanethiol (ODT). This approach tests both the stability of the silicon/organic layer interface and the passivation of the biofunctionalized surface on top of the organic layer. Microscopy and spectroscopy studies are combined to interrogate this model system before and after surface passivation.

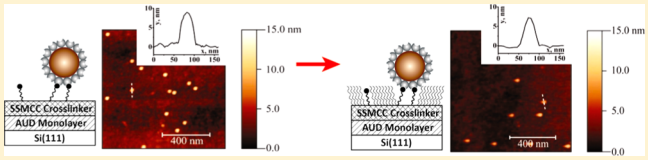

1. INTRODUCTION

In recent years, biosensors based on field effect and utilizing semiconductor substrates have become one of the most sought-after devices to detect DNA−protein interactions.[1−5] The growing interest toward these detection schemes originates from the fact that this approach is inexpensive, label-free, and allows for an all-electronic detection. Among the platforms for the biosensing field-effect transistor (FET) design, silicon has been targeted because of its attractive electronic properties that can be incorporated in most microelectronic devices.[4−6] Despite its propensity for oxidation, robust functionalization schemes for silicon can be designed to provide a stable and, if needed, oxygen-free interface if the surface of this semiconductor is modified with covalently attached monolayers.[7−9] The monolayers of functionalized alkyl groups can be grown on silicon to create the necessary barrier that can also serve for further surface modification.[10−13] Although the structure and mechanism of growth for these monolayers are very different from what is normally referred to as self-assembly, the resulting layers can be very well-ordered because of intermolecular interactions, despite the fact that the "head"-group covalently bound to the surface is not mobile,[14,15] which is different from common self-assembly on gold, for example. Thus, we will also refer to these layers and self-assembled monolayers (SAMs) as is accepted in the field of semiconductor modification.

The covalent attachment of the desired biomolecule to the functionalized SAMs is commonly achieved via a reaction with organic cross-linkers.[10,13,16] For example, thiol-modified DNA can utilize such cross-linker molecules as sulfosuccinimidyl-4-(*N*-maleimidomethyl)-cyclohexane-1-carboxylate (SSMCC) or *N*-hydroxysuccinimide (NHS). A variety of biomolecules have been successfully attached to silicon substrate, including nucleic acids,[10,13,17] glyoxylyl-modified peptites,[18] phospholipids,[19] and saccharides.[20,21] However, regardless of the efficiency of any of these reactions, there are always remaining surface reactive sites following the biomodification step.[22] These reactive sites can lead to oxidation of the underlying silicon substrate and interfere with the selective binding of the target biomolecules on top of the organic layer and thus the entire detection process. Thus, an effective chemical functionalization pathway has to be developed to neutralize these sites or to block them from participating in any other surface chemical processes following biofunctionalization.

In this work, we will use 1-octadencanethiol (ODT) as a passivating reagent. It has been used previously in this role as applied to III−V semiconductor surfaces. For example, InAs[23] and GaAs[24] can react with ODT directly via thiol chemistry and this process results in negligible oxidation while the materials retain exceptional electronic properties, as the electron mobility of the substrates has been shown to increase.[23] We will use a similar approach to passivate the surface of SAM-covered silicon following its reaction with a biomolecule to prevent further binding events.

This work employs a model system based on the Si(111) surface. It utilizes previously developed schemes to deposit a functionalized SAM on this substrate and to modify this functionalized surface with a cross-linker molecule amenable to a reaction with thiol-DNA.[10,13,17] A single-strand DNA

Received: July 12, 2012
Revised: September 27, 2012
Published: October 1, 2012

molecule (ssDNA) 10 nucleotides in length with its 3′-end modified with thiol group and 5′-end modified with biotin was covalently anchored to this surface. Further, the resulting surface was exposed to the streptavidin-coated gold nanoparticles to probe the reactivity of the surface adsorption sites based on the binding of biotin with streptavidin. Finally, we passivated this biosensor model system with ODT. The order of the last two steps has also been investigated for potential practical applications. Every step of the way, surface properties were characterized by Fourier transform infrared (FTIR) spectroscopy, X-ray photoelectron spectroscopy (XPS), atomic force microscopy (AFM), and time-of-flight secondary ion mass spectrometry (ToF-SIMS).

It is most important to realize that there are two main interfaces created during the surface modification procedure outlined here: between SAM and the silicon crystal, and between the modified SAM and the biological molecules. While we will mainly focus on the possibility to passivate the topmost functional layer for biochemical modification, we will also have to maintain the integrity of SAM/silicon interface and prevent silicon oxidation.

2. EXPERIMENTAL SECTION

2.1. Materials. 1-Amino-10-undecene (AUD) (sigma Aldrich), di-*tert*-butyl dicarbonate (Sigma Aldrich, 99%), sodium chloride (Fisher, Certified ACS), trifluoroacetic acid (TFA) (Aldrich, 99%), methylene chloride (Fisher,99.9%), petroleum ether (Fisher, Certified ACS), ethyl ether (Fisher, Laboratory grade), methanol (Fisher, 99.9%), ammonium hydroxide (Fisher, 14.8 N), hydrogen peroxide (Fisher, 30% Stabilized with Sodium Stannate, Certified), hydrochloric acid (Fisher, 37%), buffer-HF improved (Transene Company, Inc.), ammonia fluoride solution (Aldrich, 40% in water), sulfosuccinimidyl-4-(*N*-maleidomethyl)-cyclohexane-1-carboxylate (SSMCC) (Pierce), 5′-biotin-DNA-3′thiol (Integrated DNA Technologies), streptavidin gold from *Streptomyces avidinii* ∼10 nm nominal (Sigma-Aldrich, ∼2.5 A_{520} units/mL), streptavidin gold from *Streptomyces avidinii* 20 nm particle size (Sigma-Aldrich, absorption/520 nm, ≤3.0), dithiothreitol (DTT) (Fisher Biotech, Molecular Biology grade), triethanolamine (TEA) (Fisher, Certified ≥99%), ethyl acetate (EtOAc) (Fisher Scientific, Certified ACS), tris base (Fisher Scientific, Molecular Biology grade), glacial acetic acid (Fisher Scientific, Certified ACS, PLUS), disodium ethylenediaminetetraacetate (EDTA) (Fisher Scientific, Certified ACS), magnesium acetate tetrahydrate (Sigmaultra, minimum, 98%), bovine serum albumin (Sigma, electrophoresis grade), monosodium phosphate (Fisher, Certified ACS), disodium phosphate (Acros, >99%), and TWEEN 20 (Fisher, enzyme grade) were used as received. Double-polished *p*-type Si(111) crystals (>0.1 Ω cm, 500 μm ± 25 μm, Virginia Semiconductor) were used as semiconductor platforms. DI water (Resistance 18mΩ) from a Milli-Q water system (Millipore) available at the University of Delaware was used to rinse the crystals and as a solvent.

2.2. Synthesis of the *t*-Butyloxycarbonyl (*t*-BOC) Protected AUD. Five grams of 1-amino-10-undecene was dissolved in 60 mL of chloroform followed by adding a solution of 3 g of $NaHCO_3$ in 50 mL of water. Amounts of 6.45 g of sodium chloride and 7.90 g of di-*tert*-butyl dicarbonate were dissolved in a few milliliters of chloroform and then added to the mixture. The mixture was refluxed for 90 min followed by double extraction with 50 mL of ether. $MgSO_4$ was used to dry the organic extracts and then removed by filtration. Ether was removed by rotary evaporation. The obtained *t*-BOC protected AUD was purified by vacuum distillation.[10,25] The yields similar to the literature data were obtained, and the identity of the target compound was confirmed by NMR.

2.3. Preparation of Amine-Terminated SAM on Si(111). Si(111) wafer was cleaned by a modified RCA procedure.[26] At the final step, in order to form a uniform hydrogen terminated Si(111) surface, the wafer was immersed in HF buffer for 1 min and 40% ammonium fluoride for 6 min.

The preparation of an amine-terminated SAM is illustrated in Scheme 1.[26−28] Immediately after the etching step, the hydrogen terminated silicon wafer was placed in a flask with about 2 mL of *t*-BOC-protected AUD, which has been deoxygenated with dry nitrogen for at least 30 min. The flask was then immersed in an oil bath with the temperature of 110 °C, and the solution was refluxed for 2 h under the nitrogen flow. Following this reaction, the silicon wafer was rinsed with petroleum ether, dichloromethane, and methanol. The surface was then treated with 25% TFA in dichloromethane for 1 h to remove the protecting group, followed by rinsing with methylene chloride, methanol, and 10% ammonium hydroxide. The surface was finally rinsed with Milli-Q water and dried with nitrogen.

Scheme 1. Preparation of 1-Amino-10-undecene SAM on Hydrogen Terminated Si(111) Substrate

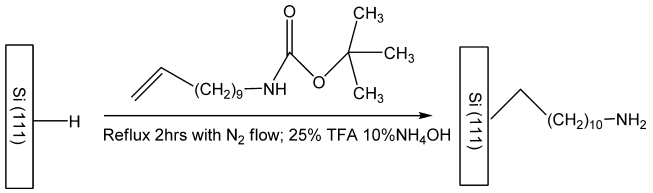

2.4. Preparation of Biotin DNA-Modified Surfaces Based on Amine Terminated SAM. The preparation of biotin DNA-modified surface is illustrated in Scheme 2.[27,28] The freshly prepared amine-terminated surfaces were incubated with 1.5 mM SSMCC in 100 mM triethanolamine (TEA) buffer (pH = 7) for 1 h. After that, the surfaces were rinsed with Milli-Q water and dried with nitrogen. The 10 nucleotides in length biotin-modified ssDNA solution of ∼10 or ∼50 μM (referred thereafter as low and high-concentration solutions, respectively) in TAE buffer (40 mM Tris, 1 mM EDTA, 20 mM acetic acid and 12.5 mM magnesium acetate) with 3′-end modified with disulfide and 5′-end modified with biotin was reduced by 100 mM DTT for 2 h. Extra DTT was removed by washing with ethyl acetate. DNA solution in TAE buffer was then spotted on the wafers and held overnight in a home-built humidity-controlled chamber. Then the surfaces were rinsed with Milli-Q water and dried with nitrogen.

Scheme 2. Preparation of Biotin DNA Modified Surface through SSMCC Cross-Linker on Amine-Terminated Si(111) Substrate

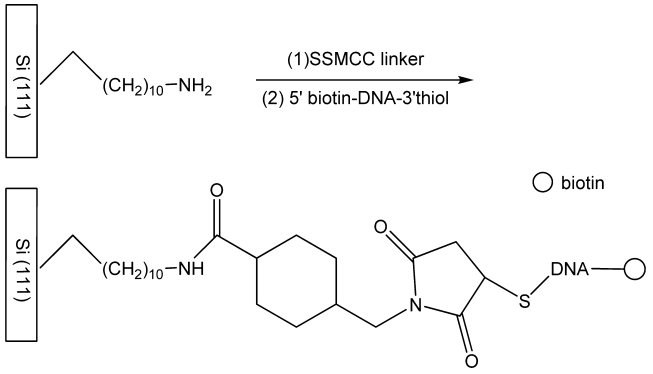

2.5. Preparation of Surfaces with Immobilized Gold Nanoparticles. The reaction of biotin-DNA-coated surfaces with streptavidin-coated gold nanoparticles is summarized in Scheme 3. The streptavidin-coated gold nanoparticle solution was first diluted 10 times with 0.01 M phosphate buffer solution (pH = 7, 0.15 M NaCl, 0.01 M sodium phosphate, 5 mg/mL albumin, and 1.1 g/mL TWEEN 20). The diluted solution was spotted on the biotin DNA modified surfaces for 2 h followed by rinsing with deionized water and drying

dx.doi.org/10.1021/la302819j | *Langmuir* 2012, 28, 15521−15528

Scheme 3. Preparation of Streptavidin-Coated Gold Nanoparticles on a Modified Si(111) Surface with Biotin-Labeled DNA

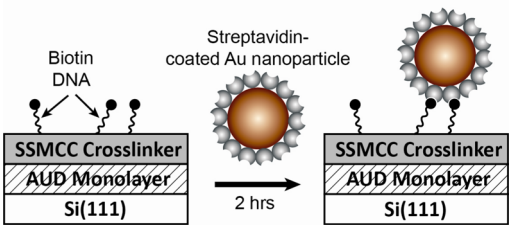

with nitrogen. The conditions were altered for the experiments with 10 and 20 nm gold nanoparticles, as described in the Supporting Information.

2.6. Passivation of the Surfaces with ODT. The surface passivation following the deposition of gold nanoparticles is shown in Scheme 4. The surface labeled with gold nanoparticles was incubated with 10 mM ODT in methanol solution overnight. The surface was then washed twice with methanol and dried with nitrogen.

Scheme 4. Passivation of the Surface Prepared According to Scheme 3 with 1-Octadecanethiol

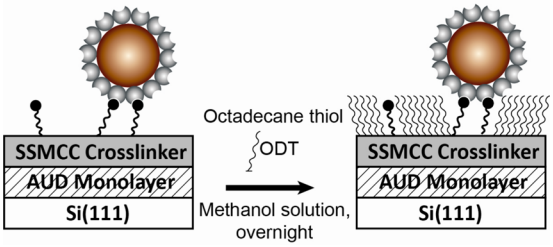

2.7. Characterization Techniques. *2.7.1. Fourier Transform Infrared Spectroscopy.* FTIR spectra were collected on Nicolet Magna-IR 560 spectrometer with a liquid-nitrogen-cooled external MCT detector. Silicon wafer was located at 60° with respect to the incoming infrared beam. All the spectra were collected in the range of 650−4000 cm^{-1} with 256 scans per spectrum at resolution 8 cm^{-1}.

2.7.2. Atomic Force Microscopy. AFM images were collected in a J-scanner tapping mode in air on a scanning probe microscope (Multimode, NanoScope V). Silicon AFM probes (Budget Sensors) with a force constant of 40 N/m and resonant frequency of 300 kHz were used. The AFM images were analyzed by using Gwyddion and NanoScope V software packages.

2.7.3. X-ray Photoelectron Spectroscopy. The XPS spectra were collected on VG ESCALAB 220i-XL electron spectrometer (VG Scientific Ltd., U.K.) with a monochromatic Al Kα X-ray source in a vacuum chamber with a background pressure of 10^{-10} Torr. Casa software was used to analyze the data.

2.7.4. Time-of-Flight Secondary-Ion Mass Spectrometry. Static ToF-SIMS spectra were collected on a ToF-SIMS IV instrument (ION-TOF, Münster, Germany) using the following conditions: (i) primary ion: Bi^{2+}, 25 keV; (ii) primary ion current: ~2.5pA in bunched mode; (iii) prebunched pulse width: 25 ns; (iv) analysis area: 500 × 500 μm^2; (v) raster resolution: 128 × 128 pixels; (vi) mass resolution: $m/\Delta m$ = 10 000. Only the negative portions of the spectra are presented in this paper to follow the sulfur signal.

3. RESULTS AND DISCUSSION

3.1. X-ray Photoelectron Spectroscopy. The XPS investigation aims at evaluating chemical identities of the surface functionalities following different modification steps. This technique can also be used for quantification of surface elements, such as, for example, carbon, oxygen, and nitrogen; however, this information is more difficult to extract in these studies, since the samples are prepared in ambient and can adsorb water, hydrocarbons, and so forth, upon transfer and mounting in the experimental setup. The XPS studies of selected systems discussed in this work are summarized in Figure 1. Spectrum 1a corresponds to the Si(111) surface

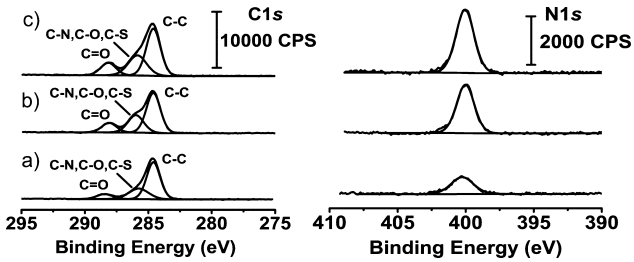

Figure 1. High-resolution C 1s and N 1s XPS of (a) DNA modified Si(111) surface; (b) gold nanoparticle labeled DNA modified Si (111) surface; and (c) ODT passivated gold-nanoparticle-labeled Si(111) surface.

modified with biotin-DNA. For C 1s spectra, the major peak is located at 284.6 eV which is attributed to C−C bond in the AUD monolayer on the silicon surface.[26,27] The peak at 285.8 eV is assigned to C−N, C−O, and C−S from the organic layers as well as DNA bases and backbones.[27] The C═O peak predominantly originating from the SSMCC cross-linker and DNA bases is located at 288.4 eV.[10,17,29] For N 1s spectra, the major peak is found at 400.3 eV and assigned to the mixture of secondary amine functionalities from organic monolayers and DNA bases.[27,30−32]

The middle set of spectra (Figure 1b) presents gold-nanoparticle-labeled DNA-modified surfaces. In C 1s spectra, the C−C major peak is located at 284.6 eV, the C−N, C−O, C−S peak is located at 286.0 eV, and the C═O peak is at 288.0 eV.[27] For N 1s spectra, the major peak is located at 400.0 eV and the intensity is increased compared to spectra in Figure 1a.[27] The binding energy for C−N, C−O, C−S, and C═O is slightly shifted comparing to the DNA modified surface, which may be caused by changes in chemical environment as well as the inhomogeneous broadening.[27,33] The intensity of the peaks for the N 1s region is doubled, and peaks corresponding to C−N, C−O, C−S, and C═O are also increased in intensity, which is consistent with the addition of gold nanoparticles modified with streptavidin, a tetramer protein.

The spectra in Figure 1c correspond to the gold-anoparticle-labeled Si(111) surface following ODT passivation. All the major peaks remain the same as in Figure 1b with minor deviation in intensity likely due to the screening by the ODT molecules that form a monolayer and an increase in a transition indicative of the C−C bond in ODT.

For all the surface modification steps, we also followed the Si 2p spectral region to confirm the integrity of the SAM/silicon interface. These studies are presented in the Supporting Information (Figure S1) and show only very minor silicon surface oxidation manifested by the SiO_x peak around 103 eV even after the multiple modification steps are performed.

Thus, chemical and semiquantitative information obtained with XPS is consistent with the successful preparation of gold nanoparticles on modified silicon surface via a biochemical modification. It also suggests that passivation with ODT following the entire procedure does not show substantial

dx.doi.org/10.1021/la302819j | Langmuir 2012, 28, 15521−15528

chemical changes on the surface that already has attached gold nanoparticles.

3.2. Fourier Transform Infrared Spectroscopy. The primary focus of the vibrational spectroscopy investigation is the C−H stretching region that will indicate the order of the surface monolayers produced, specifically by ODT, and also will allow us to estimate the portion of the surface covered by this passivating agent following biofunctionalization. Figure 2

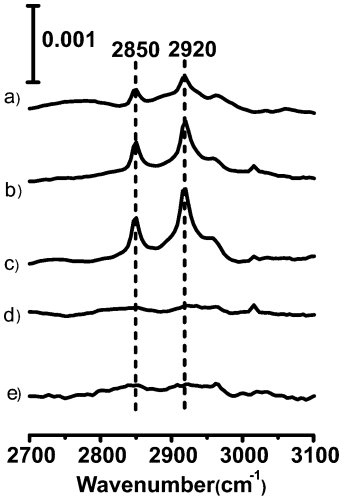

Figure 2. IR spectra of (a) high concentration of biotin-DNA-modified Si(111) surface following passivation with ODT; (b) low concentration of biotin-DNA-modified Si(111) surface following passivation with ODT; (c) ODT-passivated Si(111) surface; (d) biotin-DNA-modified Si(111) surface; (e) biotin-DNA-modified Si(111) surface labeled with gold nanoparticles (incubated with methanol solvent).

compares the FTIR spectra corresponding to the different steps of surface modification with gold nanoparticles. For all the spectra, Si(111) surface modified with AUD is used as a background. Spectrum (a) corresponds to the high concentration (∼50 μM) of biotin-DNA exposed to gold nanoparticles and passivated with ODT. Spectrum (b) is analogous to (a) but with lower concentration (∼10 μM) of DNA. Spectrum (c) follows the surface prepared the same way as in (b) but without the steps involving DNA or nanoparticle exposure; in other words, it shows the modified silicon surface with all the SSMCC functionalities on top passivated with ODT. The common feature for all three surfaces is the presence of symmetric and antisymmetric CH_2 stretching vibrations at 2850 and 2920 cm^{-1}. It is expected that for a well-ordered monolayer of alkyl chains $\nu_s(CH_2)$ would be located between 2851 and 2850 cm^{-1}, and $\nu_a(CH_2)$ between 2920 and 2918 cm^{-1}.[25,34−36] For a disordered alkyl monolayer, both symmetric and antisymmetric stretching vibrations should be shifted to higher wavenumbers: $\nu_s(CH_2)$ is expected to be located at approximately 2856−2855 cm^{-1}, and $\nu_a(CH_2)$ is expected around 2928−2925 cm^{-1}.[25,34−37] Thus, the monolayers formed following the ODT exposure in all three cases correspond to well-ordered alkyl chains within a monolayer. In addition, the intensity of the absorption peaks corresponding to the monolayers produced can give an indication of the surface concentration for ODT. Assuming that the maximum surface concentration of ODT can be obtained for a completely unmodified surface terminated with the SSMCC cross-linker, the intensity of the CH_2 absorption features can be taken as 100%. Compared to this intensity, the surface with low concentration of DNA yields the absorption intensity for the CH_2 features, which is 66% of the saturation. For high concentration DNA, this number is 27%. Thus, approximately 34% of the surface SSMCC linker groups are blocked by DNA and gold nanoparticles in a low concentration DNA sample and 73% are blocked if high-concentration of DNA is used. As expected for this type of complex system, the dependence on the DNA concentration in solution is not linear and it is likely that the exact comparison of the intensity of the infrared signal is hindered by multiple factors. However, it is clear that the high concentration of DNA leads to larger number of gold nanoparticles being adsorbed on a surface.

3.2. Atomic Force Microscopy. Figure 3 is the complete set of AFM images collected following each step of surface modification. This set of studies confirms the presence of nanoparticles, evaluates their apparent heights before and after passivation with ODT, and helps to eliminate the role of nonchemical factors in this passivation approach. Images (a) and (b) in Figure 3, hydrogen terminated Si(111) surface and amine-terminated SAM, respectively, showed a ∼0.3 nm atomic steps similar to the previously reported studies.[38,39] After further modification with SSMCC cross-linker, the surface steps are not visible anymore but the RMS roughness is still around ∼0.3 nm in image (c). Image (d) is ODT-passivated surface after the cross-linker modification, showing basically unchanged surface roughness. Images (e), (f), (g), and (k) were control experiments; no gold nanoparicles were observed on the surface either because no biotin group was available on a surface before exposure to streptavidin-coated gold nanoparticlaes (e, g, k) or because no gold nanoparticles were incorporated (f). Figure 3h follows low concentration of DNA-modified surface (∼10 μM) before exposure to gold nanoparticles. The average height of each gold nanoparticle is 8.5 ± 0.8 nm. After passivation with ODT (Figure 3i), the average height decreased to 7.5 ± 0.9 nm due to the formation of SAM. Of course, this is expected since the thickness of the passivating monolayer is expected to be on the order of a nanometer.[40] Figure 3j summarizes the studies of high concentration of DNA-modified surface (∼50 μM) followed by exposure to gold nanoparticles and ODT passivation. The average nanoparticle height was approximately 7.5 nm which is the same as for low concentration of DNA on the surface. The average concentration of gold nanoparticles was also found to be approximately five times higher on the surface with high concentration of DNA compared to that for the low concentration experiment (Figure 3i), which corresponds to the 5-fold difference in DNA concentration on the surface. Further studies of the apparent height of the nanoparticles deposited onto reactive semiconductor substrates are necessary to fully understand the role of chemical interaction in the formation of nanoparticle−surface bond and the relationship between the sizes of the nanoparticles and the length of the passivating thiols. Finally, the experiments followed in the image in Figure 3l show the system that is equivalent to that in image (j). However, in this case, attachment of DNA was first followed by passivation with ODT, and only then the surface was exposed to gold nanoparticles. As the comparison of images (j) and (l) clearly shows, the biotin DNA retains the ability to bind with streptavidin coated gold nanoparticles despite being surrounded by a passivating ODT layer. The average height of the gold nanoparticles was still approximately 7.5 nm. This last observation is especially important because it confirms that the unreacted surface sites can be effectively

dx.doi.org/10.1021/la302819j | Langmuir 2012, 28, 15521−15528

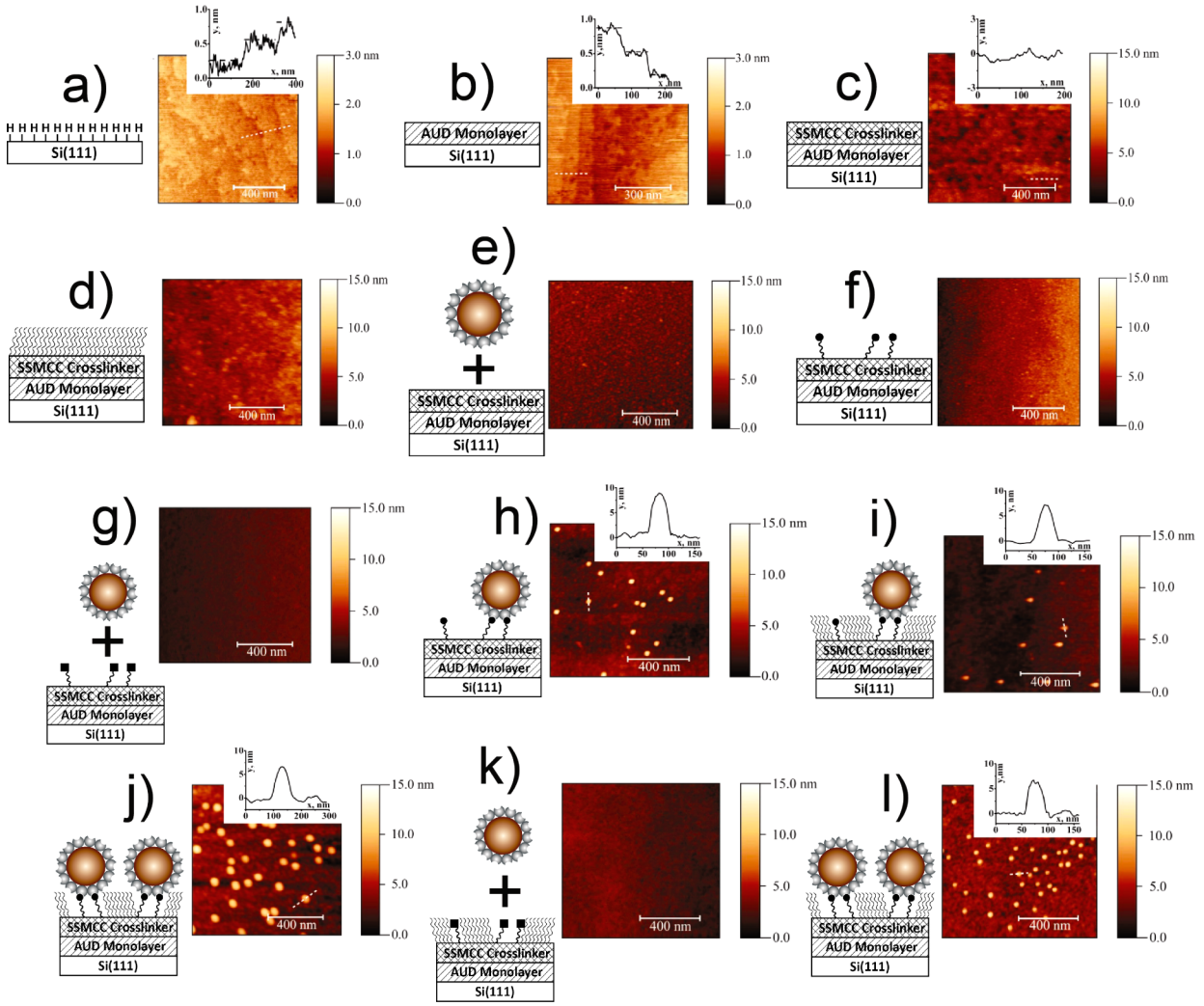

Figure 3. AFM investigation of (a) hydrogen-terminated Si(111) surface; (b) amine-terminated SAM on Si(111) surface; (c) SSMCC cross-linker based on amine-terminated SAM on Si(111) surface; (d) 1-octadecanethiol-passivated cross-linker-modified Si(111) surface; (e) sample (c) treated with streptavidin-coated gold nanoparticles; (f) biotin-DNA modified cross-linker-covered Si(111) surface; (g) control DNA-modified Si(111) surface after exposure to streptavidin-coated gold nanoparticles; (h) low concentration of biotin-DNA-modified Si(111) surface after exposure to streptavidin coated gold nanoparticles, followed by passivation with ODT; (i) (h) after passivation with 1-octadecanethiol; (j) high concentration of biotin-DNA-modified Si(111) surface after exposure to streptavidin-coated gold nanoparticles; (k) control DNA after passivation with ODT and then treated with streptavidin-coated gold nanoparticles; (l) high concentration of biotin-DNA after passivation with ODT and then treated with streptavidin-coated gold nanoparticles.

blocked by a passivating reagent without diminishing the ability of the adsorbed biological molecule to interact with incoming biomarkers. Thus, the chemical passivation approach can be used in realistic practical applications. That is, the desired biosensing platform can be prepared and the remaining surface sites can be passivated without decrease in activity for a target biochemical reaction.

We have also performed surface modification described above for extended time, up to several days, and it is clear that the saturation coverage of gold nanoparticles does not change on OTD-passivated surface. Nor do we observe any nonspecific binding as confirmed by the AFM studies in Figure 3g and k. It is also important, however, to evaluate how robust the specific binding scheme is in our system. We have performed a set of preliminary studies that compared the reactions of 20 and 10 nm gold nanoparticles presented in Figure S2 in the Supporting Information. The surface prepared as described above but with 20 nm gold nanoparticles coated with streptavidin exhibits the same number of particles per unit area as the surface prepared with 10 nm nanoparticles, passivated with ODT and then exposed to the 20 nm gold nanoparticles coated with streptavidin for 4 days. We do observe the exchange of 10 nm nanoparticles to 20 nm nanoparticles; however, the total number of gold nanoparticles does not seem to change to within our experimental uncertainty. The kinetics of this type of process is a subject of further investigation. It will depend on a number of factors including steric interaction of streptavidin-coated nanoparticles with the surface.[41] Of course, the kinetics of binding biotin and streptavidin are related to the surface coverage of the biotin group[42] and there is also a competitive reaction between surface-bound 10 nm streptavidin coated gold nanoparticles and the streptavidin on 20 nm gold nanoparticles.[43]

3.4. Time-of-Flight Secondary-Ion Mass Spectrometry. The chemical identity of sulfur-containing functionalities and the quantification of the sulfur-containing groups on a

dx.doi.org/10.1021/la302819j | *Langmuir* 2012, 28, 15521−15528

surface should be extremely helpful in understanding the passivation process described here. However, due to low sensitivity of the sulfur in XPS as well as to the overlap of the S 2p signal with Si 2s signals,[44] we chose to use a very sensitive technique, time-of-flight secondary-ion mass spectrometry (ToF-SIMS), to obtain information about this element.

Figure 4 displays the negative ion spectra following main modification steps of the Si(111) surface. Figure 4a is the

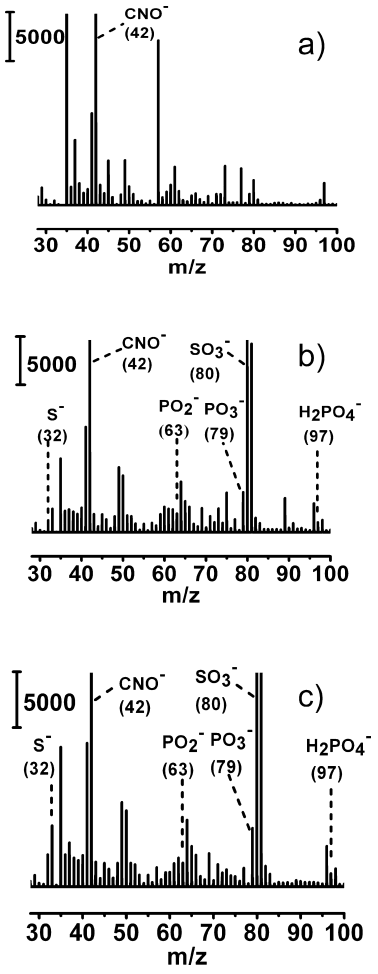

Figure 4. TOF-SIMS studies of (a) *t*-BOC-protected AUD monolayer on Si(111) calibrated by oxygen peak; (b) biotin-DNA-modified Si(111) surface; (c) biotin-DNA-modified Si(111) surface after passivation with ODT. Only negatively charged ions are shown.

spectrum of *t*-BOC protected AUD on silicon. This spectrum provides the starting point for comparison with biofunctionalized surfaces. Compared to Figure 4a, the spectrum in Figure 4b, taken following the attachment of thiol-DNA molecules (at low concentration, ~10 μM) to the surface shows the presence of S^- (m/z = 32), PO_2^- (m/z = 63), and PO_3^-(m/z=79) ions, which indicates the presence of DNA molecules. After passivating the rest of the reaction sites with ODT, PO_2^- (m/z = 63) and PO_3^-(m/z = 79) signals are still present in the spectrum shown in Figure 4c. Sulfur (m/z = 32) signal increased dramatically, which corresponds to ODT reaction. Figure 5 zooms in on the sulfur spectral region. Using O_2 signature as a comparison, it is easy to see that sulfur is virtually absent from the surface covered with the protected AUD monolayer. Sulfur signal increases dramatically following attachment of thiol-DNA. Finally, as the surface is further

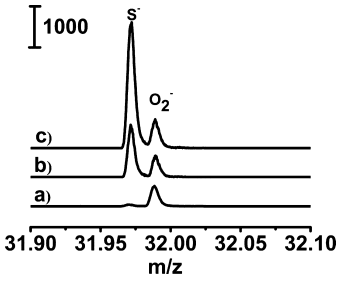

Figure 5. TOF-SIMS investigation of sulfur region: (a) *t*-BOC AUD monolayer on Si(111); (b) biotin-DNA-modified Si(111); (c) biotin-DNA-modified Si(111) after passivation with ODT. Negatively charged ions are shown.

exposed to ODT for chemical passivation, sulfur signal further increases by a factor of 2.7 compared to the spectrum in Figure 5b. Although ToF-SIMS results can only be treated as semiquantitative, this increase corresponds perfectly to the XPS and infrared analyses presented above. In particular, this observation is in excellent agreement with the infrared data that suggested that 34% of the surface participates in a reaction with biotin-DNA and further with streptavidin-coated gold nanoparticles, which leaves about 66% of surface reactive sites to be modified with ODT.

4. CONCLUSIONS

In this work, 1-octadecanethiol was used to passivate the unreacted surface sites for the biosensor model system. The test system was built on a Si(111) surface modified with AUD, further reacted with a chemical linker and then with a thiol biotin-DNA. This model surface was reacted with streptavidin-coated gold nanoparticles to confirm the binding efficiency and the role of alkyl thiol as a passivating reagent was explored. Because of the complexity of the systems produced, we had to employ a number of analytical spectroscopic and microscopic techniques following each step in surface modification. XPS study proved the successful labeling of the DNA-modified surface with streptavidin-coated gold nanoparticles, as the intensities of the indicative N 1s and C 1s peaks increased. In infrared spectroscopy studies, we observed increasing intensities of CH_2 symmetric and antisymmetric stretching vibrations at 2850 and 2920 cm^{-1}, respectively, following passivation of the surface with ODT. The positions of these bands indicated that the reaction of ODT resulted in a well-ordered monolayer and the intensity of these spectral features allowed for quantification of the surface sites that were unreacted following DNA binding and gold nanoparticle exposure. The AFM images confirmed the integrity of the nanoparticles following their binding to the surface, eliminated nonchemical reasons for binding, and followed the 1 nm decrease of apparent height of the nanoparticles after surface passivation with ODT. Finally, ToF-SIMS investigation focused on the role of sulfur in chemical bonding both for the biochemical sensing element and for passivation reagent and allowed for a semiquantitative analysis of the coverage, which appeared to be fully consistent with XPS and IR studies. The XPS studies that followed Si 2p spectral region in XPS confirmed that during all the steps described above only minor oxidation at the Si/SAM interface is observed. Thus, we successfully passivated the biosensor model system with organic ODT molecules and confirmed that in the case studied the process of passivation does not inhibit the ability of

dx.doi.org/10.1021/la302819j | *Langmuir* 2012, 28, 15521−15528

biofunctionalized surfaces to interact with incoming biological molecules, making this approach useful for practical applications.

■ ASSOCIATED CONTENT

Supporting Information

XPS analysis of the Si 2p spectral region for all the silicon surface modification steps described in this paper and a comparison of the AFM studies of 20 nm gold nanoparticles coated with streptavidin on a surface modified with biotin-DNA with the silicon surface modified with biotin-DNA, saturated with 10 nm gold nanoparticles coated with streptavidin, passivated with ODT and exposed to 20 nm gold nanoparticles coated with streptavidin for 4 days to follow saturation/exchange reaction. This material is available free of charge via the Internet at http://pubs.acs.org.

■ AUTHOR INFORMATION

Corresponding Author

*Telephone: (302) 831-1969. Fax: (302) 831-6335. E-mail: andrewt@udel.edu.

Notes

The authors declare no competing financial interest.

■ ACKNOWLEDGMENTS

This work was partially supported by the National Science Foundation (CHE-1057374). Y.L. acknowledges the helpful discussion and assistance with AFM and XPS studies from Ms. Fangyuan Tian and Mr. Timothy Miller, and the input on DNA chemistry from Ms. Jennifer Codding and Professor Colin Thorpe, Department of Chemistry and Biochemistry, University of Delaware. The help of Dr. Holt Bui with ToF-SIMS and XPS measurements at the Surface Analysis Facility (Department of Chemistry and Biochemistry, University of Delaware) is also gratefully acknowledged.

■ REFERENCES

(1) Souteyrand, E.; Cloarec, J. P.; Martin, J. R.; Wilson, C.; Lawrence, I.; Mikkelsen, S.; Lawrence, M. F. Direct Detection of the Hybridization of Synthetic Homo-Oligomer DNA Sequences by Field Effect. *J. Phys. Chem. B* **1997**, *101*, 2980−2985.

(2) Souteyrand, E.; Martin, J. R.; Martelet, C. Direct-Detection of Biomolecules by Electrochemical Impedance Measurements. *Sens. Actuators, B* **1994**, *20*, 63−69.

(3) Han, Y.; Offenhausser, A.; Ingebrandt, S. Detection of DNA Hybridization by a Field-Effect Transistor with Covalently Attached Catcher Molecules. *Surf. Interface Anal.* **2006**, *38*, 176−181.

(4) Kim, A.; Ah, C. S.; Yu, H. Y.; Yang, J.-H.; Baek, I.-B.; Ahn, C.-G.; Park, C. W.; Jun, M. S.; Lee, S. Ultrasensitive, Label-Free, and Real-Time Immunodetection Using Silicon Field-Effect Transistors. *Appl. Phys. Lett.* **2007**, *91*.

(5) Bunimovich, Y. L.; Ge, G. L.; Beverly, K. C.; Ries, R. S.; Hood, L.; Heath, J. R. Electrochemically Programmed, Spatially Selective Biofunctionalization of Silicon Wires. *Langmuir* **2004**, *20*, 10630−10638.

(6) Cai, W.; Peck, J. R.; van der Weide, D. W.; Hamers, R. J. Direct Electrical Detection of Hybridization at DNA-Modified Silicon Surfaces. *Biosens. Bioelectron.* **2004**, *19*, 1013−1019.

(7) Ishizaki, T.; Saito, N.; SunHyung, L.; Ishida, K.; Takai, O. Study of Alkyl Organic Monolayers with Different Molecular Chain Lengths Directly Attached to Silicon. *Langmuir* **2006**, *22*, 9962−9966.

(8) Linford, M. R.; Fenter, P.; Eisenberger, P. M.; Chidsey, C. E. D. Alkyl Monolayers on Silicon Prepared from 1-Alkenes and Hydrogen-Terminated Silicon. *J. Am. Chem. Soc.* **1995**, *117*, 3145−3155.

(9) Sung, M. M.; Kluth, G. J.; Yauw, O. W.; Maboudian, R. Thermal Behavior of Alkyl Monolayers on Silicon Surfaces. *Langmuir* **1997**, *13*, 6164−6168.

(10) Strother, T.; Cai, W.; Zhao, X. S.; Hamers, R. J.; Smith, L. M. Synthesis and Characterization of DNA-Modified Silicon (111) Surfaces. *J. Am. Chem. Soc.* **2000**, *122*, 1205−1209.

(11) Bocking, T.; James, M.; Coster, H. G. L.; Chilcott, T. C.; Barrow, K. D. Structural Characterization of Organic Multilayers on Silicon(111) Formed by Immobilization of Molecular Films on Functionalized Si-C Linked Monolayers. *Langmuir* **2004**, *20*, 9227−9235.

(12) Yang, W. S.; Butler, J. E.; Russell, J. N.; Hamers, R. J. Direct Electrical Detection of Antigen-Antibody Binding on Diamond and Silicon Substrates Using Electrical Impedance Spectroscopy. *Analyst* **2007**, *132*, 296−306.

(13) Strother, T.; Hamers, R. J.; Smith, L. M. Covalent Attachment of Oligodeoxyribonucleotides to Amine-Modified Si (001) Surfaces. *Nucleic Acids Res.* **2000**, *28*, 3535−3541.

(14) Blanchard, P.-Y.; Aleveque, O.; Boisard, S.; Gautier, C.; El-Ghayoury, A.; Le Derf, F.; Breton, T.; Levillain, E. Intermolecular Interactions in Self-Assembled Monolayers of Tetrathiafulvalene Derivatives. *Phys. Chem. Chem. Phys.* **2011**, *13*, 2118−2120.

(15) Ulman, A. Formation and Structure of Self-Assembled Monolayers. *Chem. Rev.* **1996**, *96*, 1533−1554.

(16) Wagner, P.; Nock, S.; Spudich, J. A.; Volkmuth, W. D.; Chu, S.; Cicero, R. L.; Wade, C. P.; Linford, M. R.; Chidsey, C. E. D. Bioreactive Self-Assembled Monolayers on Hydrogen-Passivated Si(111) as a New Class of Atomically Flat Substrates for Biological Scanning Probe Microscopy. *J. Struct. Biol.* **1997**, *119*, 189−201.

(17) Lin, Z.; Strother, T.; Cai, W.; Cao, X. P.; Smith, L. M.; Hamers, R. J. DNA Attachment and Hybridization at the Silicon (100) Surface. *Langmuir* **2002**, *18*, 788−796.

(18) Coffinier, Y.; Olivier, C.; Perzyna, A.; Grandidier, B.; Wallart, X.; Durand, J. O.; Melnyk, G.; Stievenard, D. Semicarbazide-Functionalized Si(111) Surfaces for the Site-Specific Immobilization of Peptides. *Langmuir* **2005**, *21*, 1489−1496.

(19) Cunin, F.; Milhiet, P. E.; Anglin, E.; Sailor, M. J.; Espenel, C.; Le Grimellec, C.; Brunel, D.; Devoisselle, J. M. Continuous Planar Phospholipid Bilayer Supported on Porous Silicon Thin Film Reflector. *Ultramicroscopy* **2007**, *107*, 1048−1052.

(20) de Smet, L.; Pukin, A. V.; Stork, G. A.; de Vos, C. H. R.; Visser, G. M.; Zuilhof, H.; Sudholter, E. J. R. Syntheses of Alkenylated Carbohydrate Derivatives toward the Preparation of Monolayers on Silicon Surfaces. *Carbohydr. Res.* **2004**, *339*, 2599−2605.

(21) de Smet, L.; Zuilhof, H.; Sudholter, E. J. R.; Lie, L. H.; Houlton, A.; Horrocks, B. R. Mechanism of the Hydrosilylation Reaction of Alkenes at Porous Silicon: Experimental and Computational Deuterium Labeling Studies. *J. Phys. Chem. B* **2005**, *109*, 12020−12031.

(22) Sarveswaran, K.; Hu, W.; Huber, P. W.; Bernstein, G. H.; Lieberman, M. Deposition of DNA Rafts on Cationic Sams on Silicon 100. *Langmuir* **2006**, *22*, 11279−11283.

(23) Hang, Q.; Wang, F.; Carpenter, P. D.; Zemlyanov, D.; Zakharov, D.; Stach, E. A.; Buhro, W. E.; Janes, D. B. Role of Molecular Surface Passivation in Electrical Transport Properties of Inas Nanowires. *Nano Lett.* **2008**, *8*, 49−55.

(24) Budz, H. A.; Biesinger, M. C.; LaPierre, R. R. Passivation of Gaas by Octadecanethiol Self-Assembled Monolayers Deposited from Liquid and Vapor Phases. *J. Vac. Sci. Technol. B* **2009**, *27*, 637−648.

(25) Sieval, A. B.; Demirel, A. L.; Nissink, J. W. M.; Linford, M. R.; van der Maas, J. H.; de Jeu, W. H.; Zuilhof, H.; Sudholter, E. J. R. Highly Stable Si-C Linked Functionalized Monolayers on the Silicon (100) Surface. *Langmuir* **1998**, *14*, 1759−1768.

(26) Zhang, X.; Teplyakov, A. V. Adsorption of C-60 Buckminster Fullerenes on an 11-Amino-1-Undecene-Covered Si(111) Substrate. *Langmuir* **2008**, *24*, 810−820.

(27) Zhang, X.; Kumar, S.; Chen, J.; Teplyakov, A. V. Covalent Attachment of Shape-Restricted DNA Molecules on Amine-Functionalized Si(111) Surface. *Surf. Sci.* **2009**, *603*, 2445−2457.

(28) Zhang, X. C.; Antonopoulos, I. H.; Kumar, S.; Chen, J.; Teplyakov, A. V. Tuning the Geometry of Shape-Restricted DNA Molecules on the Functionalized Si(111). *Appl. Surf. Sci.* **2009**, *256*, 815−818.
(29) Bertani, P.; Wen, X. J.; Lu, W. Surface Functionalization of Hydrogen-Terminated Si for Biosensing Applications. *J. Electron. Mater.* **2012**, *41*, 830−836.
(30) Petrovykh, D. Y.; Kimura-Suda, H.; Whitman, L. J.; Tarlov, M. J. Quantitative Analysis and Characterization of DNA Immobilized on Gold. *J. Am. Chem. Soc.* **2003**, *125*, 5219−5226.
(31) Vilar, M. R.; do Rego, A. M. B.; Ferraria, A. M.; Jugnet, Y.; Nogues, C.; Peled, D.; Naaman, R. Interaction of Self-Assembled Monolayers of DNA with Electrons: Hreels and Xps Studies. *J. Phys. Chem. B* **2008**, *112*, 6957−6964.
(32) Leftwich, T. R.; Teplyakov, A. V. Calibration of Computationally Predicted N 1s Binding Energies by Comparison with X-Ray Photoelectron Spectroscopy Measurements. *J. Electron Spectrosc. Relat. Phenom.* **2009**, *175*, 31−40.
(33) Verpoort, F.; Dedoncker, G.; Bossuyt, A. R.; Fiermans, L.; Verdonck, L. Angle-Resolved and Depth Profiling Xps Investigation of a Monolayer Niobium Oxide Catalyst. *J. Electron Spectrosc. Relat. Phenom.* **1995**, *73*, 271−281.
(34) Sieval, A. B.; Linke, R.; Heij, G.; Meijer, G.; Zuilhof, H.; Sudholter, E. J. R. Amino-Terminated Organic Monolayers on Hydrogen-Terminated Silicon Surfaces. *Langmuir* **2001**, *17*, 7554−7559.
(35) Perring, M.; Dutta, S.; Arafat, S.; Mitchell, M.; Kenis, P. J. A.; Bowden, N. B. Simple Methods for the Direct Assembly, Functionalization, and Patterning of Acid-Terminated Monolayers on Si(111). *Langmuir* **2005**, *21*, 10537−10544.
(36) Tian, F. Y.; Yang, D.; Opila, R. L.; Teplyakov, A. V. Chemical and Electrical Passivation of Si(111) Surfaces. *Appl. Surf. Sci.* **2012**, *258*, 3019−3026.
(37) Snyder, R. G.; Strauss, H. L.; Elliger, C. A. C-H Stretching Modes and the Structure of Normal-Alkyl Chains 0.1. Long, Disordered Chains. *J. Phys. Chem.* **1982**, *86*, 5145−5150.
(38) Zhong, Y. L.; Bernasek, S. L. Mild and Efficient Functionalization of Hydrogen-Terminated Si(111) Via Sonochemical Activated Hydrosilylation. *J. Am. Chem. Soc.* **2011**, *133*, 8118−8121.
(39) Allongue, P.; de Villeneuve, C. H.; Morin, S.; Boukherroub, R.; Wayner, D. D. M. The Preparation of Flat H-Si(111) Surfaces in 40% NH_4F Revisited. *Electrochim. Acta* **2000**, *45*, 4591−4598.
(40) Tian, F. Y.; Ni, C. Y.; Teplyakov, A. V. Integrity of Functional Self-Assembled Monolayers on Hydrogen-Terminated Silicon-on-Insulator Wafers. *Appl. Surf. Sci.* **2010**, *257*, 1314−1318.
(41) Bonanno, L. M.; DeLouise, L. A. Steric Crowding Effects on Target Detection in an Affinity Biosensor. *Langmuir* **2007**, *23*, 5817−5823.
(42) Zhou, C.; Qi, K.; Wooley, K. L.; Walker, A. V. Time-of-Flight Secondary Ion Mass Spectrometry, Fluorescence Microscopy and Scanning Electron Microscopy: Combined Tools for Monitoring the Process of Patterning and Layer-by-Layer Assembly of Synthetic and Biological Materials. *Colloids Surf., B* **2008**, *65*, 85−91.
(43) Jung, L. S.; Nelson, K. E.; Stayton, P. S.; Campbell, C. T. Binding and Dissociation Kinetics of Wild-Type and Mutant Streptavidins on Mixed Biotin-Containing Alkylthiolate Monolayers. *Langmuir* **2000**, *16*, 9421−9432.
(44) Coulter, S. K.; Schwartz, M. P.; Hamers, R. J. Sulfur Atoms as Tethers for Selective Attachment of Aromatic Molecules to Silicon(001) Surfaces. *J. Phys. Chem. B* **2001**, *105*, 3079−3087.